DNA methylation is involved in acclimation to iron-deficiency in rice (*Oryza sativa*)

Shuo Sun[1,2,†] [iD], Jiamei Zhu[1,2,†], Runze Guo[1,2], James Whelan[2,3] [iD] and Huixia Shou[1,2,4,]*

[1]*State Key Laboratory of Plant Physiology and Biochemistry, College of Life Sciences, Zhejiang University, Hangzhou, Zhejiang 310058, P.R. China,*
[2]*The Provincial International Science and Technology Cooperation Base on Engineering Biology, International Campus of Zhejiang University, Haining, Zhejiang 314400, P.R. China,*
[3]*Australian Research Council Centre of Excellence in Plant Energy Biology, Department of Animal, Plant and Soil Science, School of Life Science, La Trobe University, Victoria 3086, Australia, and*
[4]*Hainan Institute, Zhejiang University, Sanya 572025, China*

SUMMARY

Iron (Fe) is an essential micronutrient in plants, and Fe limitation significantly affects plant growth, yield and food quality. While many studies have reported the transcriptomic profile and pursue molecular mechanism in response to Fe limitation, little is known if epigenetic factors play a role in response to Fe-deficiency. In this study, whole-genome bisulfite sequencing analysis, high-throughput RNA-Seq of mRNA, small RNA and transposable element (TE) expression with root and shoot organs of rice seedlings under Fe-sufficient and Fe-deficient conditions were performed. The results showed that widespread hypermethylation, especially for the CHH context, occurred after Fe-deficiency. Integrative analysis of methylation and transcriptome revealed that the transcript abundance of Fe-deficiency-induced genes was negatively correlated with nearby TEs and positively with the 24-nucleotide siRNAs. The ability of methylation to affect the physiology and molecular response to Fe-deficiency was tested using an exogenous DNA methyltransferase inhibitor (5-azacytidine), and genetically using a mutant for domains rearranged methyltransferase 2 (DRM2), that lacks CHH methylation. Both approaches resulted in decreased growth and Fe content in rice plants. Thus, alterations in specific methylation patterns, directed by siRNAs, play an important role in acclimation of rice to Fe-deficient conditions. Furthermore, comparison with other reports suggests this may be a universal mechanism to acclimate to limited nutrient availability.

Keywords: *Oryza sativa*, iron (Fe)-deficiency, DNA methylation, transcriptome, siRNA, transposable element.

INTRODUCTION

Iron (Fe) is an essential micronutrient for the survival of all organisms. It serves as a cofactor for more than 300 enzymes and plays an essential role in many fundamental biological processes, such as photosynthesis, mitochondrial respiration, nitrogen assimilation, hormone biosynthesis, osmoprotection and pathogen defense (Hansch and Mendel, 2009). Fe-deficiency not only affects the healthy growth of plants, but also leads to Fe-deficiency in humans with plant-based diets, and in severe cases it can cause Fe-deficiency anemia (Clark *et al.*, 2014; Sankaran and Weiss, 2015). Fe is present in aerated soils as ferric Fe (Fe^{3+}), which is practically insoluble at the physiological pH range under aerobic conditions (Guerinot and

Yi, 1994). To overcome Fe-deficiency, plants have evolved two strategies to optimize Fe acquisition and uptake. Non-graminaceous plants use a reduction-based mechanism (Strategy I), while graminaceous plants use a chelation-based mechanism (Strategy II; Kobayashi *et al.*, 2014; Kobayashi and Nishizawa, 2012). Rice (*Oryza sativa*) is unique among graminaceous plants because it can also employ the Strategy I Fe-uptake mechanism under flooded conditions (Bughio *et al.*, 2002; Cheng *et al.*, 2007; Ishimaru *et al.*, 2006). In the past two decades, a large number of genes involved in Fe uptake and homeostasis have been identified, including those that encode transcription factors (TFs) for regulating expression of genes whose transcript abundance change in response to

Fe availability, encoding enzymes for synthesis of mugineic acids (MAs), and transporters of MA-Fe(III) or Fe (II) in rice (Bughio *et al.*, 2002; Cheng *et al.*, 2007; Inoue *et al.*, 2003, 2009; Kobayashi *et al.*, 2007, 2014; Ogo *et al.*, 2006, 2008; Wang *et al.*, 2013, 2020; Zheng *et al.*, 2010). Despite the considerable advances in understanding of transcriptional and post-transcriptional mechanisms of plant responses to Fe-deficiency, the involvement or changes in epigenetic components of the cell to Fe-deficiency have not been investigated in plants.

Cytosine DNA methylation (mC) is an epigenetic feature with key roles in genome stability and expression in mammals and plants (He and Ecker, 2015; Huff and Zilberman, 2014; Schmitz *et al.*, 2019; Zhang *et al.*, 2018). It is involved in the transcriptional silencing of transposable elements (TEs), thus contributing to the preservation of genome integrity, as well as in the regulation of expression of specific genes (Law and Jacobsen, 2010; Rodrigues and Zilberman, 2015). Methylation of cytosine occurs in three sequence contexts, CG and CHG (symmetric) and CHH (asymmetric); where H = C, A or T. Methylation in each context is catalyzed by a specific family of DNA methyltransferases (Law and Jacobsen, 2010). Maintenance of CG and CHG methylation is regulated by DNA methyltransferase1 (MET1) in a semi-conservative manner during DNA replication (Kankel *et al.*, 2003), and chromomethylase 3 (CMT3), which is targeted to DNA by recognizing H3K9 methylation (Bartee *et al.*, 2001; Lindroth *et al.*, 2001). *De novo* CHH methylation is generated after DNA replication, and established by small [typically 24 nucleotides (nts)] interfering with the RNA-directed DNA methylation (RdDM) pathway (Mirouze and Paszkowski, 2011). In RdDM, RNA polymerase IV and Dicer-like proteins are responsible for siRNA biogenesis, while RNA polymerase IV, AGO (argonaute) 4/6 and the methyltransferase domains rearranged methyltransferase 2 (DRM2) are involved in siRNA-guided DNA methylation (Kawashima and Berger, 2014; Law and Jacobsen, 2010; Matzke *et al.*, 2015; Matzke and Mosher, 2014; Nuthikattu *et al.*, 2013). The DNA methylation status is maintained not only by DNA methyltransferases but also by several DNA demethylases, such as ROS1 (repressor of silencing 1), DME (Demeter), DML2 (Demeter-like 2) and DML3 (Liu *et al.*, 2018; Ortega-Galisteo *et al.*, 2008; Penterman *et al.*, 2007).

When plants are exposed to adverse environments, such as changes in temperature, light intensity, nutrient and water availability, plants 'record' the unfavorable events through changes in DNA methylation pattern (Kinoshita and Seki, 2014). A study on the spatio-temporal dynamics of mC in rice grown under inorganic phosphate (Pi) limitation and re-supply showed that Pi starvation-induced changes in mC in the CHH context preferentially localized in TEs close to (approximately 205 bp) genes whose transcripts are increased in abundance (Secco *et al.*, 2015). Moreover, these changes in mC occurred after the increase in transcript abundance of adjacent genes, and could partially be propagated through mitosis. In addition, these changes in methylation pattern were mostly independent of DCL3a (Dicer-like 3a), which is a key factor involved in the canonical RdDM pathway. Another study identified widespread differences in CG and non-CG methylation marks between cadmium (Cd)-exposed and Cd-free rice genomes (Feng *et al.*, 2016). Compared with wild-type, mutation of MET1 and DRM2, which are required for maintaining methylation, resulted in lower transcript levels of genes encoding metal transporters, Cd-detoxifying proteins and metal-related TFs under Cd stress. A global DNA methylation inhibitor, 5-azacytidine, reduced general DNA methylation levels of these Cd-responsive genes, but growth of rice seedlings and Cd accumulation increased in rice plant. DNA methylation maps in two representative soybean genotypes with different Pi efficiencies reveal that the DNA methylation levels were slightly higher under Pi limitation in both genotypes, and dynamic methylation alterations in TE regions in the CHH methylation context occurs corresponding with changes in the abundance of siRNA under Pi-deficiency conditions (Chu *et al.*, 2020). For another nutrient zinc (Zn), genome-wide DNA methylation changed upon prolonged Zn-deficiency in Arabidopsis roots and it was demonstrated that differential DNA methylation in the CG and CHG, but not CHH context, was related to the upregulation of some Zn-deficiency-induced genes (Chen *et al.*, 2018).

Here, DNA methylomes, transcriptomes of protein-coding genes and TEs and siRNA profiles were determined from rice roots and shoots under Fe-sufficient and Fe-deficient conditions. Widespread hypermethylated regions, especially in the CHH context in response to Fe-deficiency, were observed. Except for siRNA changes, DNA methyltransferase and other RdDM components showed no significant changes in transcript abundance under Fe-deficiency. This study reveals the dynamics of DNA methylation under Fe-deficiency in rice, and suggests a mobile siRNA-dependent RdDM mechanism in response to nutrient limitation.

RESULTS

Features of rice DNA methylome under Fe-deficient and Fe-sufficient conditions

To investigate the effects of Fe-deficiency on genomic DNA (gDNA) methylation patterns in rice, whole-genome bisulfite sequencing (BS) was performed on rice roots and shoots of 10-day-old seedlings under Fe-sufficient and Fe-deficient conditions (Figure 1a). Fe-deficiency was confirmed by the increased transcript abundance of four genes (Figure S1), leaf chlorosis and reduced Fe content
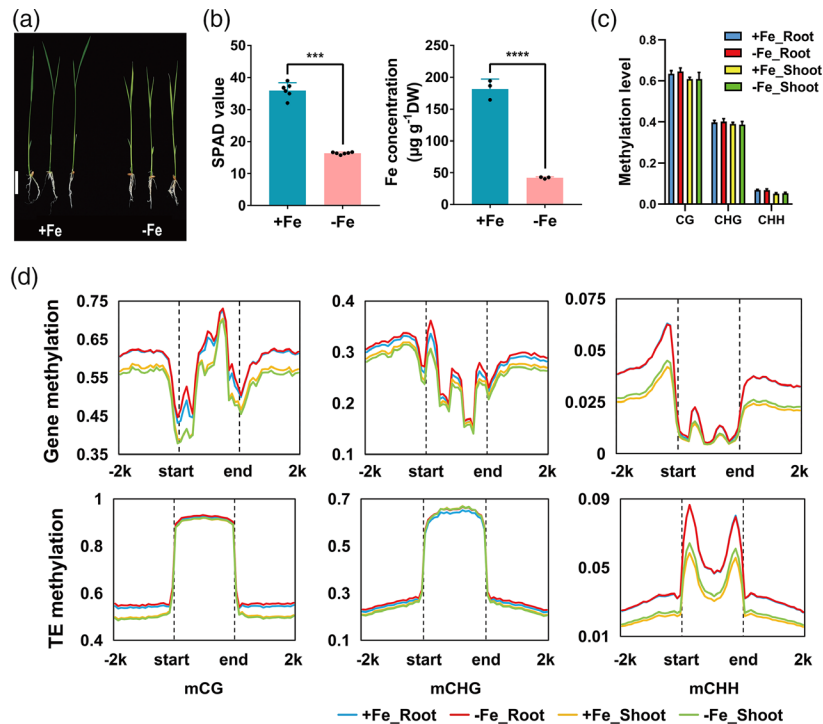
Figure 1. Characterization of the methylomes of rice.
(a) Rice grown under Fe-sufficient and -deficient conditions (scale bar: 3 cm).
(b) Soil Plant Analysis Development (SPAD) values representing chlorophyll content of leaves and shoot Fe content. Data are shown as the mean and standard deviation (SD) ($n = 6$). One-way analysis of variance (ANOVA) followed by Tukey test; ***$P < 0.001$; ****$P < 0.0001$.
(c) Histogram of methylation frequencies on the *y*-axis for different levels of CG, CHG and CHH methylation (*x*-axis) in rice roots and shoots under Fe-sufficient and -deficient conditions.
(d) DNA methylation profiles of mCG, mCHG and mCHH surrounding genes and transposable elements (TEs; within 2 kb) in rice roots and shoots under Fe-sufficient and -deficient conditions.

(Figure 1b). After removing the adaptors and filtering the low-quality reads (Q30 < 90%), the average number of clean reads was 34.75 million, and the BS conversion rates were > 99.21% (Table S1a). Mapping reads from the 12 samples resulted on average with 27.31 million reads (78.60%) uniquely mapped to the rice reference genome (MSU_v7.0; Table S1b). This resulted in a sequencing depth of > 18 ×, and at least 78.72% of the sequenced sites were covered by > 10 × per sample (Table S1c). Analysis of genomic methylation of CG, CHG and CHH in rice roots and shoots under Fe-sufficient or Fe-deficient conditions revealed that an average of 49.78, 30.52 and 19.7% mCs occurred at CG, CHG and CHH sites respectively (Table S2). The average methylation levels of CG, CHG and CHH were about 64.0, 40.0 and 6.8% in roots, and 60.9, 38.9 and 5.3% in shoots, respectively (Figure 1c), which is similar to previous reports in rice (Feng *et al.*, 2016; Li *et al.*, 2012). Fe-deficiency led to < 1% variation in three contexts at the whole-genome level (Figure 1c; Table S2). Moreover, the level of DNA methylation under sufficient and deficient conditions in 5′- and 3′-flanking regions of protein-coding genes was at a higher level in roots than in shoots in all three types of DNA methylation (Figure 1d).

Fe-deficiency-induced CHH methylation

To examine the response of DNA methylation changes in response to Fe-deficiency, differentially methylated regions (DMRs; > twofold change, $P < 0.05$) between Fe-sufficient and Fe-deficient were determined. In total, 4259 and 5703 DMRs were identified in the 2-kb regions next to expressed genes in the roots and shoots under Fe-deficiency, respectively (Table S3). Most DMRs occurred in the CHH contexts in both roots and shoots (Figure 2a). The number of hyper CHH-DMRs was about twice that of hypo CHH-DMRs in both roots and shoots. The numbers of CG-DMRs and CHG-DMRs detected in the shoots were more than eight-fold and twofold compared with roots, respectively. Ninety-five percent of DMR-associated genes (DMGs) are associated with only one context of DMR in both roots and shoots (Figure 2b). However, an interesting phenomenon is that the CHG-DMGs almost exclusively overlapped with CG-DMGs (approximately 99%) in roots, but a similar result was not observed in the shoots. To obtain an understanding of the biological functions of different contexts of DMGs, a Gene Ontology (GO) category analysis was performed. Regardless of whether DMGs are hypermethylated
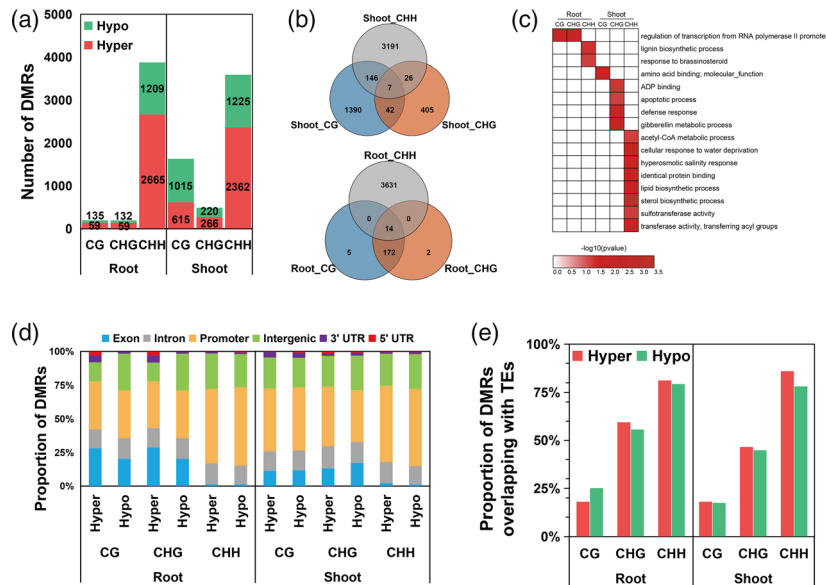
Figure 2. Characterization of differentially methylated regions (DMRs) in different cytosine contexts.
(a) Number of DMRs near to protein-coding genes (within 2 kb) in rice roots and shoots.
(b) Overlap of differentially methylated genes (DMGs) with different methylation contexts.
(c) Gene Ontology (GO) analysis of DMGs from different methylation contexts ($P < 0.05$).
(d) Genomic compositions of DMRs surrounding genes.
(e) Proportion of DMRs overlapping with transposable elements (TEs).

or hypomethylated, it was found that those CG-DMGs and CHG-DMGs were primarily associated with regulation of transcription from RNA polymerase II promoter in roots, while CHH-DMGs were related to lignin biosynthetic process and response to brassinosteroid in roots (Figure 2c). Consistent with the low overlap of different contexts of DMGs, the functions of different contexts of DMGs in shoots also differed. For instance, a large number of CG-DMGs in shoots were mainly enriched in the function of amino acid binding, while CHG-DMGs in shoots were associated with ADP binding, apoptotic process, defense response and gibberellin metabolic process. Moreover, CHH-DMGs in shoots were mainly related to lipid and sterol biosynthetic process, transferase activity, acetyl-CoA metabolic process and hyperosmotic salinity response. Compared with CG-DMRs and CHG-DMRs, CHH-DMRs were distributed in the promoter regions (Figure 2d), and highly overlapped with TE bodies ($> 80\%$) in both roots and shoots (Figure 2e). Altogether, the majority of the Fe-deficiency-induced DMRs close to genes are preferentially in the CHH context and located in the promoter regions, and almost exclusively overlap with TEs.

Interconnection of DNA methylome and RNA transcriptome

To determine if the DMRs associated with TEs under Fe-deficiency impact gene expression, RNA-Seq was performed using the same materials as those used for methylome

analysis. In total, 682 and 146 differentially expressed genes (DEGs) were identified in the roots and shoots, respectively [$\log_2 FC| > 1$, false discovery rate (FDR) < 0.05]. The number of genes that were altered was consistent with previous studies (Kobayashi and Nishizawa, 2012; Kobayashi *et al.*, 2019; Wang *et al.*, 2020). Differentially expressed TEs (DETEs) near DEGs were 63% (428/682) and 68% (99/146) DEGs in the 2-kb regions flanking the DETEs in the roots and shoots, respectively (Figure 3a). In contrast, only 5 and 1% of randomly selected genes with DETEs nearby in the roots and shoots, respectively. GO enrichment analysis revealed genes involved in the categories of 'response to Fe ion', 'Fe ion homeostasis' and 'Fe ion transport' were enriched in both DEGs and genes surrounding with DETEs in both roots and shoots (Figure 3b). Analysis of the correlation between the expression fold changes of DEGs and TEs in the 2-kb regions flanking the DEGs (Figure 3c) showed that the expression of DEGs is highly negatively correlated with their nearby TEs in both roots ($R^2 = 0.66$, $P = 5.7e - 19$) and shoots ($R^2 = 0.71$, $P = 3.1e - 49$). To investigate whether DEGs with DETEs within 2 kb are regulated by specific TFs and epigenetic factors, binding factor enrichment analysis was performed, and it was found that H3K27me3 and bZIP23 are over-represented surrounding DEGs in both roots and shoots ($P < 0.001$; Figure 3d). In *Arabidopsis thaliana*, FIT-dependent Fe acquisition genes, IRT1 and FRO2, as well as FIT itself are direct targets of PRC2-mediated H3K27me3 (Park *et al.*, 2019). The *clf* mutant, which lacks the
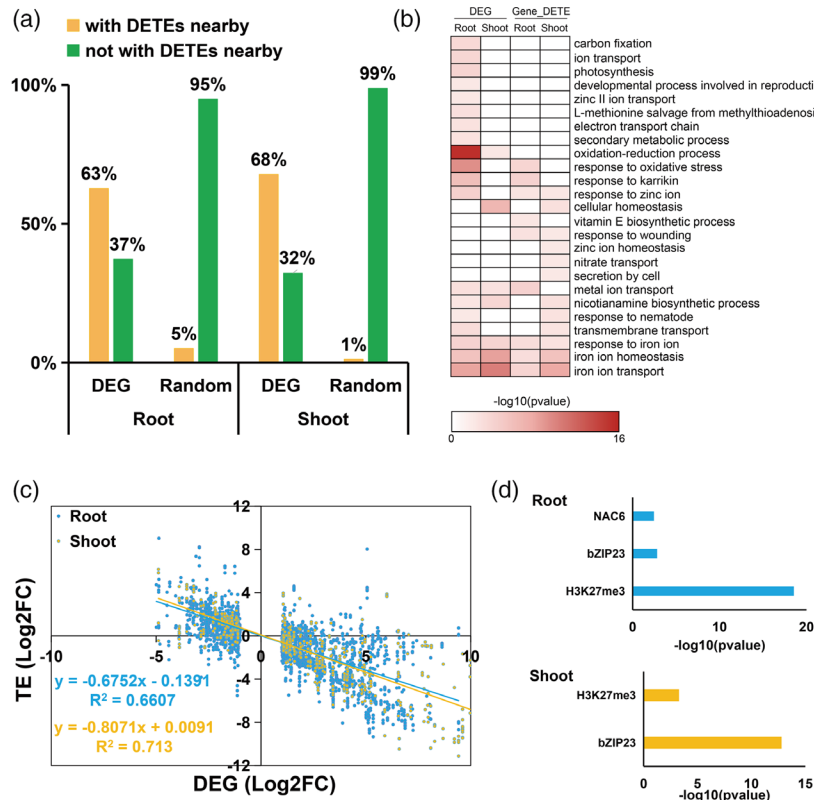
Figure 3. Analysis of rice Fe-deficient transcriptome.

(a) Differentially expressed genes [DEGs; |$\log_2$FC| > 1, false discovery rate (FDR) < 0.05] are significantly associated with differentially expressed transposable elements (DETEs; |$\log_2$FC| > 1, FDR < 0.05) nearby (within 2 kb) as compared with randomly selected genes in both roots and shoots (P < 0.001).

(b) Gene Ontology (GO) enrichment analysis of DEGs and genes with nearby DETEs (P < 0.05).

(c) Equation of linear regression of fold-changes on $\log_2$-scale of the Fe-deficiency-induced DEGs and their nearby transposable elements (TEs; within 2 kb).

(d) Binding factor enrichment analysis indicated the transcription factors (TFs) and epigenetic factors whose bindings over-represented surrounding Fe-deficiency-responsive DEGs with DETEs nearby (P < 0.001).

predominant H3K27 tri-methyltransferase, was observed to be more tolerant to Fe-deficiency than wild-type (Park *et al.*, 2019). This suggests that there may be a similar histone modification mechanism involved in response to Fe homeostasis in rice.

To explore any links between methylation changes on transcriptional changes, Fe-deficiency-responsive DMGs associated with DEGs were identified. Altogether, 86 and 31 DMGs overlapped with DEGs, including 83/86 and 25/31 that were CHH-DMGs, in roots and shoots, respectively (Figure 4a). Interestingly, although only a small amount of Fe-deficiency-induced genes were hypermethylated, two core TFs, IRO2 and OsbHLH156, which positively regulate most of the Fe-deficiency-inducible genes, were both hypermethylated in the promoter regions in the roots or shoots (Figure 4b,c). In addition, Fe-transporter-encoding genes or other Fe-related genes were also detected as DMGs in the roots (MTK2, SAM2, NAAT1, NRAMP1, TOM1, FDH1) and shoots (YSL2, IRT2, NAS3; Figure 4c; Table S4). To demonstrate the effect of DNA methylation changes on gene expression changes, the number of DMGs that

showed positive or negative correlation between changes of promoter methylation and gene expression according to functional classification were determined. Almost all the DMGs related to Fe-binding/transport/homeostasis showed positive correlation between promoter methylation and gene expression (Figure 4c,d). Altogether, Fe-deficiency-induced genes are generally hypermethylated in the CHH context and negatively associated with nearby TEs, especially for Fe-signaling pathway genes.

Twenty-four nucleotide siRNA clusters are associated with increased DNA methylation

Small RNAs can direct *de novo* DNA methylation at their target loci through RdDM pathways (Law and Jacobsen, 2010; Mosher and Melnyk, 2010). Small RNA expression profiles from the same material as methylome analysis were determined by high-throughput deep sequencing. It was found that the 24-nt class was the most abundant group of small RNAs in roots and shoots based on their distribution in length (Figure 5a). To characterize the effects of siRNAs on genome methylation patterns and
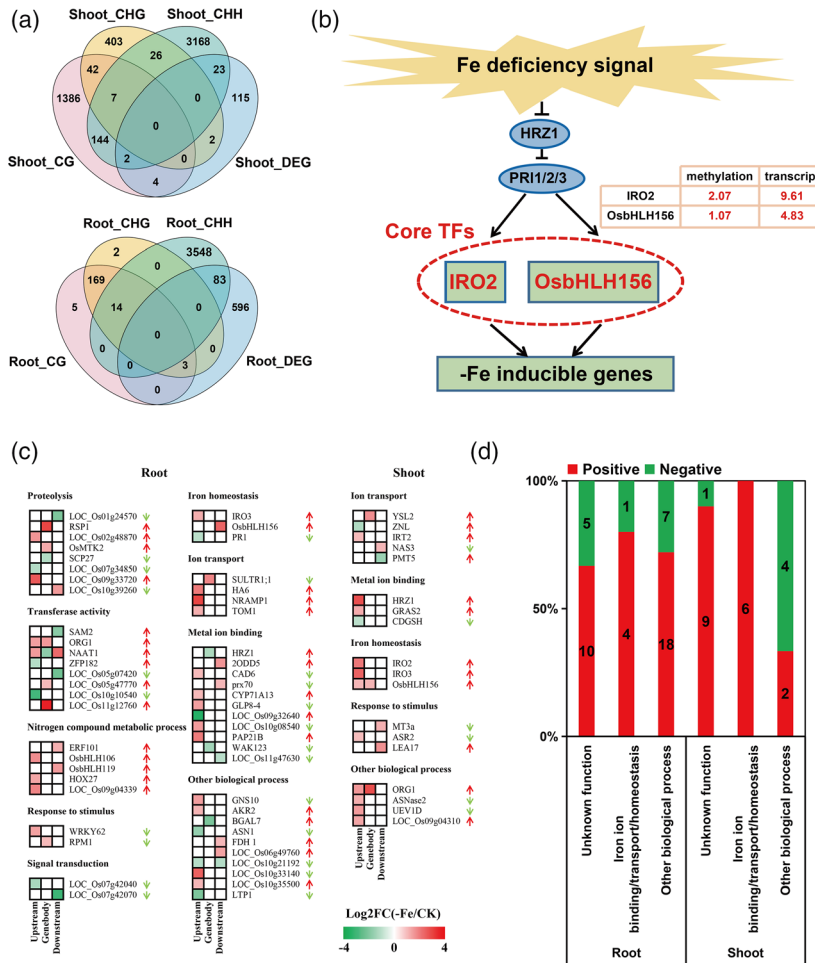
Figure 4. Combinational analyses of genes that changed in DNA methylation and genes that changed in transcript abundance.

(a) Venn diagrams display the association between differentially methylated regions (DMR)-associated genes (DMGs) in the three contexts, and Fe-deficiency-induced differentially expressed genes (DEGs) in rice roots and shoots.

(b) Core transcription factors (TFs) in the upstream of Fe-deficiency signaling pathway. The level of CHH methylation and transcription changes of IRO2 and OsbHLH156 in the shoots are shown as $\log_2$ (−Fe/+Fe) values on the right.

(c) Functionally clustering of the different genes expressing under Fe-deficiency stress. Heat map represents the methylation levels of individual Fe-deficiency-responsive genes in the gene upstream (2 kb), gene-body and downstream regions (2 kb). Arrows indicate up or down transcription level in rice roots and shoots.

(d) Statistics on the number of DMGs whose promoter methylation change is positive or negative with the gene expression change.

gene expression, differential siRNA clusters between samples under Fe-sufficient and Fe-deficient conditions were determined ($|\log_2 FC| > 1$, $P < 0.05$). As expected, 24-nt siRNAs changed the most (Figure 5b).

As RdDM is guided by 24-nt siRNAs (Law and Jacobsen, 2010; Matzke *et al.*, 2015; Wambui Mbichi *et al.*, 2020), the features of the regions that overlapped with the 24-nt siRNA-covered regions were examined. It was found that over 62% of Fe-deficiency-induced hyper CHH-DMRs overlapped with the 24-nt siRNA clusters in both roots and shoots (Figure 5c). Only 16% of randomly selected genomic regions overlapped with the 24-nt siRNA clusters, indicating that Fe-limitation-induced hyper CHH-DMRs are significantly associated with siRNAs ($P < 0.01$). Consistent with the CHH methylation pattern in the 2-kb regions

flanking to expressed genes or TEs (Figure 1d), the abundance of 24-nt siRNAs in TE body was much higher than that in the 2 kb upstream or downstream of TE (Figure 5d). Furthermore, the expression levels of Fe-deficiency-related DEGs have a highly positive correlation with their nearby 24-nt siRNA clusters (in the 2-kb regions flanking to the DEGs) in both roots ($R^2 = 0.51$, $P = 7.1e − 3$) and shoots ($R^2 = 0.36$, $P = 1.6e − 3$; Figure 5e). To further explore the connection between siRNA-mediated DNA methylation and Fe-deficiency-induced DNA hypermethylation, changes in 24-nt siRNA enrichment at Fe-deficiency-induced hyper CHH-DMRs were analyzed (Figure 5f). The results showed that siRNA levels were significantly increased at hyper CHH-DMRs after Fe-deficiency in both roots and shoots ($P < 0.001$).
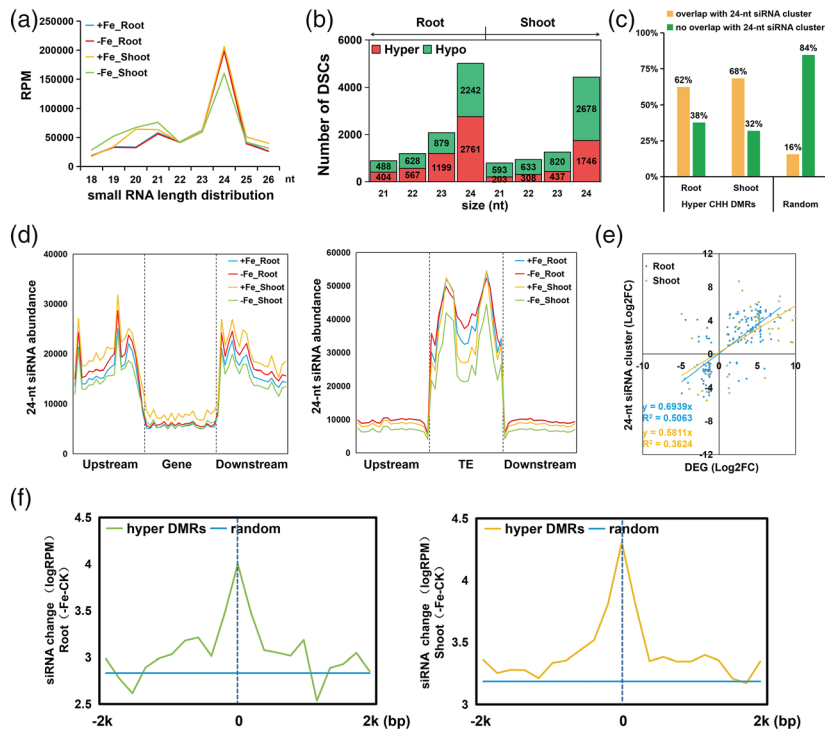
Figure 5. Correlation between the change of siRNA clusters and DNA hypermethylation responsive to Fe-deficiency.

(a) Size distribution of sequenced small RNAs.

(b) Number of differentially expressed siRNA clusters of different lengths ($|\log_2 FC| > 1$, $P < 0.05$).

(c) Hyper CHH differentially methylated regions (DMRs) are significantly associated with 24-nucleotide (nt) siRNA clusters as compared with random genomic regions ($P < 0.01$).

(d) Abundance of 24-nt siRNAs surrounding genes and transposable elements (TEs; within 2 kb) in rice roots and shoots under Fe-sufficient and -deficient conditions.

(e) Equation of linear regression of fold-changes on $\log_2$-scale of the Fe-deficiency-induced differentially expressed genes (DEGs) and their nearby 24-nt siRNA clusters.

(f) Change of 24-nt siRNA abundance surrounding hyper-DMRs and random genomic regions on average in rice roots and shoots.

DNA demethylation represses the growth and Fe accumulation of rice

To investigate whether DNA methylation can affect Fe-deficiency signaling and/or Fe-deficiency-related phenotypes, rice plants grown under Fe-sufficient and Fe-deficient conditions were treated with a DNA methylation inhibitor (5-aza-2-deoxycytidine, Aza). The growth response to Fe-deficiency was assessed by measuring shoot and root heights (Figure 6a). The exogenous application of Aza resulted in significant shoot growth inhibition under both Fe-sufficient and Fe-deficient conditions. To confirm the effect of Aza on DNA methylation, two Fe-deficient induction genes, Os*bHLH156* and *IRO2*, were tested for DNA methylation using BS-polymerase chain reaction (BS-PCR). As expected, treatment with Aza led to a lower degree of DNA methylation of these genes (Figure 6b). To determine the effect of DNA demethylation on Fe homeostasis, Fe content of rice shoots was also measured. The results showed that the exogenous Aza application resulted in a significant decrease of shoot Fe concentrations under Fe-

deficient conditions (Figure 6c). The effect of Aza on the expression of Fe-deficiency-induced gene expression was tested. The transcript abundance of *OsZIP1* was used as an internal marker gene as it was shown to be induced by the application of Aza and supressed by DNA methylation (Feng *et al.*, 2016). A similar pattern was observed in this study, *OsZIP1* was induced in the roots by the addition of Aza (Figure 6c). However, the expression of two core TFs involved in the Fe-deficiency signaling pathway, *IRO2* and *OsbHLH156*, were repressed in the roots or shoots by the application of Aza under Fe-deficient conditions. Besides, several other genes that are induced under Fe-deficient conditions including *NAAT1*, *NAS2*, *YSL15* and *HRZ1* were also found to be repressed by the application of Aza under Fe-deficient conditions in the roots (Figure S2).

Due to the toxic effects of Aza, the specificity of this effect was tested using a genetic approach. It is reported that the loss of function of DRM2 can significantly reduce the level of CHH methylation in whole rice genome (Tan
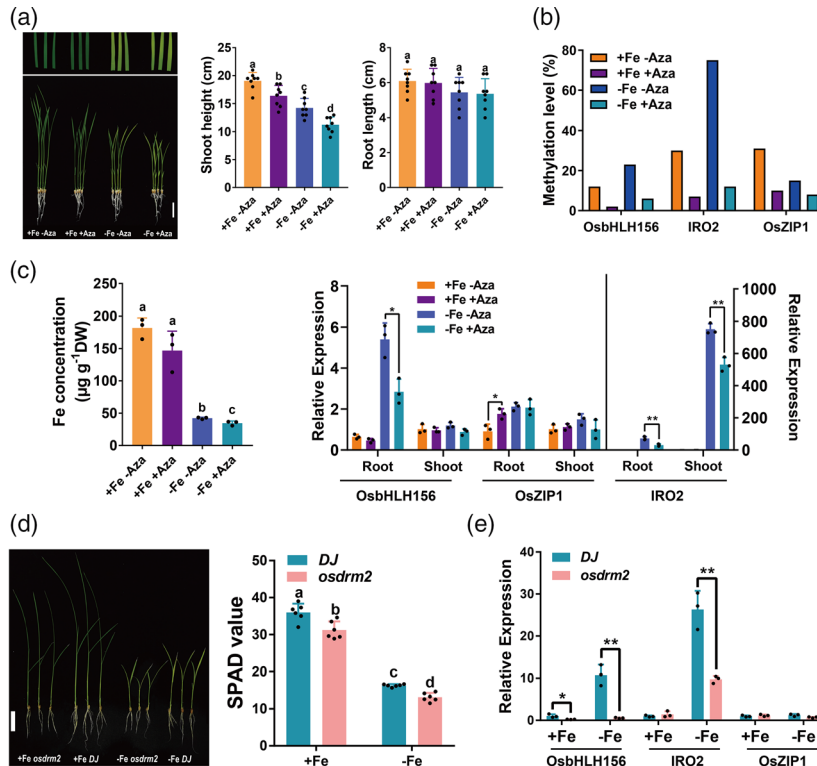
Figure 6. Effects of repression of DNA methylation in rice roots and shoots under Fe-sufficient and -deficient conditions.

(a) Phenotype of 3-day-old rice seedlings under Fe-sufficient (+Fe) or -deficient (−Fe) conditions and/or treated with 20 μM DNA methyltransferase inhibitor (5-aza-2-deoxycytidine, Aza) for 7 days (scale bar: 3 cm). Shoot heights and root lengths of rice seedlings were measured.

(b) DNA methylation levels of selected genes (*OsbHLH156/IRO2/OsZIP1*).

(c) Fe content in rice shoots and transcript abundance of selected genes.

(d) Phenotype of 10-day-old wild-type and *osdrm2* mutant rice seedlings and SPAD value of leaves under Fe-sufficient or -deficient conditions (scale bar: 3 cm).

(e) Relative expression of *OsbHLH156, IRO2* and *OsZIP1* in rice roots under Fe-sufficient and -deficient conditions. Vertical bars represent SD of the mean of three biological replicates. *P < 0.05; **P < 0.01; one-way ANOVA followed by Tukey test.

et al., 2016). Therefore, we obtained wild-type and the T-DNA insertion mutant of *osdrm2* in a Dongjin genetic background as used in a previous study (Tan *et al.*, 2016). Phenotypic analysis showed that the loss of function of DRM2 led to the repression of plant growth (Figure 6d). In addition, Soil Plant Analysis Development (SPAD) values of wild-type and *osdrm2* leaves indicated that the content of Fe in *osdrm2* is significantly lower than in the wild-type. Moreover, the induction of expression of the core Fe-responsive TFs OsbHLH156 and IRO2 by Fe-deficiency was repressed in the *osdrm2* roots. Thus, combining the chemical and genetic approaches supports a functional role for changes in methylation under Fe-deficiency (Figure 6e).

Expression of known genes relevant to DNA methylation are not responsive to Fe-deficiency

DNA methyltransferase(s) play a basic role in maintaining DNA methylation and DNA demethylation (Teerawanichpan *et al.*, 2004; Yamauchi *et al.*, 2008, 2009). The rice genome contains 10 genes that encode DNA methyltransferase

members that can be phylogenetically classified into CMT, MET (DNMT1-like), DNMT2-like and DRM (DNMT3-like) clades (Ahmad *et al.*, 2014; Chen and Zhou, 2013; Qian *et al.*, 2014). To understand the response of DNA methyltransferases to Fe-deficient stress, the members of CMT, MET, DNMT2-like and DRM families were identified based on rice genome annotation and homology alignment. As shown in Table S5, the expression of most methyltransferases in the roots was significantly higher than that in the shoots. The transcript abundance of most of these genes was not affected by Fe-deficiency in rice, except *ROS1A* (repressor of silencing 1A), a demethylase-coding gene responsible for DNA demethylation (Agius *et al.*, 2006), was weakly repressed by Fe-deficiency in the roots (P < 0.05; FDR > 0.05). The expression of RNA-dependent RNA polymerase (RDR) protein genes, AGO4a and AGO4b, which have been reported to play roles in generating the 24-nt sRNAs (Wang *et al.*, 2014; Zhang and Zhu, 2011), genes involved in chromatin remodeling, histone modification and polycomb repressive complex 2 proteins were also monitored. As a whole, the expression levels of nearly
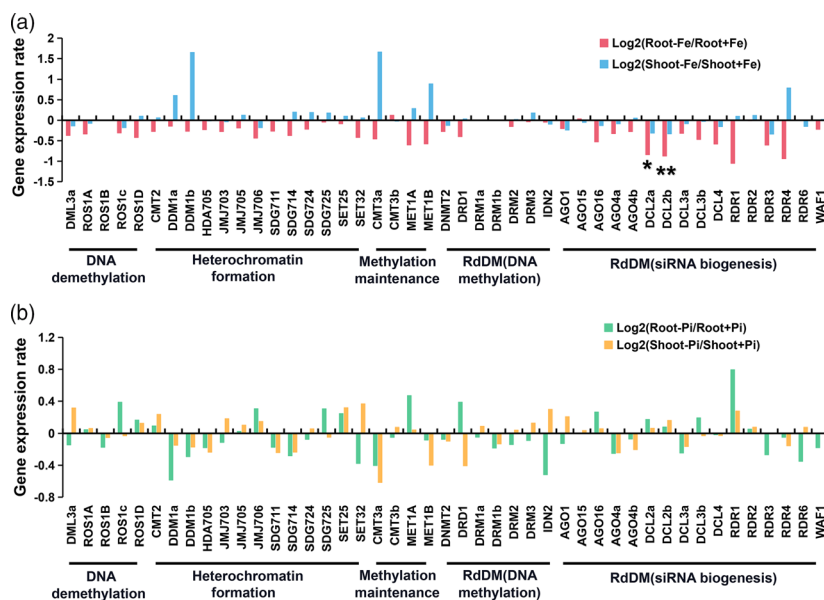
Figure 7. Transcript abundance of genes encoding proteins involved in epigenetic modification in Fe- and Pi-deficient rice.
DNA methylation/demethylation, heterochromatin formation and RNA-directed DNA methylation (RdDM) components reported in rice were included. The transcriptional levels of genes differentially induced by Fe-deficiency (a) and Pi-deficiency (b) were determined by published RNA-Seq datasets. Data are represented as the ratio of $\log_2$ [fragments per kilobase per million reads (FPKM) values (μtreated/μCK)]. *FDR < 0.05; **FDR < 0.01.

all of these genes in the roots were much higher than those in the shoots, which was consistent with the higher methylation level of the roots (Figures 1 and 7). This indicates that methyltransferases and RdDM play an important role in the difference of methylation level between different tissues. No difference in these genes was observed after Fe-deficiency (Figure 7a), except for DCL2a and DCL2b (FDR < 0.05), which are responsible for processing double-stranded RNA into 21 and 22 nt siRNAs (Parent *et al.*, 2015). Therefore, we speculated that the local differential methylation induced by Fe-deficiency is not mediated by the known methyltransferases and canonical RdDM components, or that post-transcriptional regulation of these activities occurs.

DISCUSSION

During the past decade, a variety of studies on transcriptomes and functional analysis have greatly enriched our understanding of how plants maintain Fe homeostasis under different Fe availability (Kobayashi and Nishizawa, 2012; Kobayashi *et al.*, 2019). However, little is known about the potential role of changes in the epigenome in response to Fe-deficiency. Here, we generated a single-base resolution map of DNA methylation for rice roots and shoots under Fe-sufficient and Fe-deficient conditions. Although the rice plants under Fe-sufficient or Fe-deficient conditions had similar genomic cytosine methylation levels, local variations were observed for the specific DNA methylation in the context of CHH, where Fe-deficiency increased in overall DNA methylation levels (Figures 1 and

2). In addition, application of the methyltransferase inhibitor Aza led to the repression of genes involved in the Fe signaling pathway and the decrease of Fe content in rice under Fe-deficiency (Figure 6). Aza is known to be toxic, and a genetic approach was used to confirm the role of methylation in the Fe-deficiency response. The rice mutant *osdrm2* whose CHH methylation level at a whole-genome level is significantly lower than the wild-type (Tan *et al.*, 2016), exhibited growth inhibition and reduced SPAD values under Fe-sufficient and -deficient conditions. While not many Fe-deficiency-induced genes were hypermethylated after Fe-deficiency, two core TFs that regulate the Fe-deficiency response, IRO2 and OsbHLH156, were hypermethylated (Figure 4b). Taken together, we propose that the methylation changes of *IRO2* and Os*bHLH156* are an important regulatory feature that impacts the majority of the Fe-deficiency responses as they are required for the induction of many downstream targets.

A similar picture has also been found in the previous study related to Pi-deficiency in rice (Secco *et al.*, 2015). In that study, researchers used time-course experiments, and proposed that changes in transcription occurred before changes in DNA methylation levels. Thus, the differential DNA methylation may be caused by the induction of gene transcription. In addition, genes related to DNA methylation did not change significantly under Fe- and Pi-deficient conditions (Figure 7; Table S5), and the differential methylation regions near Fe- or Pi-deficiency-induced genes are both mainly in the CHH context and overlap with TE. These characteristics indicate that the response mechanism to

environmental nutrient limitation appears similar. The hypothesis needs to be further verified using the small RNA expression profile under Pi- and other nutrient-deficient conditions.

The enrichment of 24-nt siRNAs is an important indicator of RdDM activity (Law and Jacobsen, 2010; Matzke *et al.*, 2015). In this study, more 24-nt siRNAs were recruited in the TE regions adjacent to Fe-deficiency-induced genes, and the transcript abundance of TEs was suppressed by Fe-deficiency (Figure 5). Meanwhile, a higher CHH methylation level was observed in the 24-nt siRNA regions and TE bodies, indicating that RdDM activity may be the mechanism that underlies the specific changes that occur in methylation in the Fe-deficiency response. However, the transcript abundance of those genes encoding RDR1-6, AGO4/6 and DCL3, which are responsible for the generation of 24-nt siRNAs, did not change under Fe-deficiency. In this study, it was found that more 23-nt and 24-nt hyper siRNA clusters were identified in the roots than shoots, while more hypo siRNA clusters were detected in the shoots than roots (Figure 5b). Many studies have shown that 23–24-nt siRNAs are the major long-distance mobile siRNAs especially for the interactions between shoot and root (Martınez *et al.*, 2016; Molnar *et al.*, 2010; Pagliarani and Gambino, 2019; Tamiru *et al.*, 2018). Thus, it is possible that the change of siRNA cluster abundance may depend on the long-distance transport of siRNA between shoot and root to alter gene expression.

The combined evidence suggests that rice acclimates to Fe-deficiency by increasing the CHH methylation level adjacent to specific genes in the genome. This local hypermethylation does not depend on the change in transcript abundance of genes encoding the canonical RdDM-related enzymes, but may rely on the movement of 24-nt mobile siRNAs between roots and shoots. The 24-nt siRNAs can be recruited at TEs to increase the DNA methylation level to inhibit the negative effect of TEs on the expression of adjacent genes, especially for the key regulators in the Fe-deficient response pathway. Through this mechanism, the induction of Fe-deficiency genes can be enhanced and maintained over long time periods to optimize uptake of Fe under Fe-deficient conditions. Combined with the reported Pi-deficiency-induced changes in methylation and transcriptome (Secco *et al.*, 2015), it is speculated that this may be a universal mechanism for rice to adapt to nutrient-deficient stress. These findings broaden our understanding of the role of DNA methylation and small RNA in plant response(s) to abiotic stress.

EXPERIMENTAL PROCEDURES

Plant materials and growth conditions

Rice (*O. sativa* L. cv Nipponbare) was used in this study. Seeds were pre-germinated for 2 days in tap water, and then grown under the conditions of day/night temperature of 30°C/22°C and a 12 h photoperiod, 200 μmol photons m^{-2} sec^{-1}. The hydroponic nutrient solution supplied with Fe (+Fe) or without Fe (−Fe), containing 0.51 mM K_2SO_4, 1.64 mM $MgSO_4$, 0.32 mM NaH_2PO_4, 1.0 mM $CaCl_2$, 1.43 mM NH_4NO_3, 9 μM $MnCl_2$, 0.13 μM $CuSO_4$, 0.02 μM H_3BO_3, 0.08 μM $(NH_4)_6Mo_7O_{24}$, 0.15 μM $ZnSO_4$, 0.25 mM Na_2SiO_3 and 125 μm EDTA-Fe(II) (if supplied). The pH of the solution was adjusted to 5.5–5.6, and the solution was changed every 3 days. Rice roots and shoots grown hydroponically for 10 days after germination with or without Fe were separately collected from seedlings, and each sample was performed with three biological replicates.

Rice (*O. sativa* L. ssp. Japonica 'DongJin') plants were used in this study. T-DNA insertion lines of *osdrm2* (PFG_3A-04110) were obtained from the Postech rice mutant database (http://www.postech.ac.kr/life/pfg/risd/). The insertion of *osdrm2* mutant was by the primers 3A-04110-P1 and 3A-04110-P2. The primers used for genotyping are listed in Table S6.

gDNA extraction and MethylC-Seq library generation

gDNA was extracted from rice roots and shoots using the Universal Genomic DNA Extraction Kit (TaKaRa, Dalian, China). DNA concentration was measured and adjusted to the same level. For constructing MethylC-Seq libraries, 1 μg gDNA was sonicated into 200–500-bp fragments. After 3′-A addition and adaptor ligation, the DNA fragments were subjected to sodium bisulfite conversion using the ZYMO EZ DNA Methylation-Gold kit (ZYMO, Irvine, CA, USA). Insert fragments with different sizes were purified by 2% agarose gel electrophoresis. The final libraries were generated by PCR amplification. Bisulfite libraries were analyzed by an Agilent-t2100 Bioanalyzer (Agilent Technology, Shanghai, China) and quantified by QPCR (Agilent QPCR NGS Library Quantification Kit). The construction of bisulfite libraries and paired-end sequencing using Illumina HiSeqTM 2500 (Illumina, San Diego, CA, USA) were performed at Beijing Biomarker Technology (Beijing, China).

BS-Seq data processing and analysis

Raw 150-nt paired-end reads were subjected to quality control (QC) filters using FASTQC (http://www.bioinformatics.babraham.ac.uk/projects/fastqc/) and trimmed using Trimmomatic v0.39 (Bolger *et al.*, 2014). The remaining high-quality trimmed reads were aligned to rice reference genome (MSU_v7.0) using Bismark (Krueger and Andrews, 2011). Duplicated reads resulting from PCR were removed from each of the methylomes. The methylation level of an individual cytosine was calculated from the number of sequenced cytosines divided by the total read depth [i.e. mC/(mC + non-mC)]. Only sites that covered more than four mapped reads were considered.

Total RNA isolation and library preparation

The total RNA from the rice roots and shoots was isolated and purified using TRIzol reagent (Invitrogen, Carlsbad, CA, USA) following the manufacturer's procedure. The RNA amount and purity of each sample was quantified using NanoDrop ND-1000 (NanoDrop, Wilmington, DE, USA). The RNA integrity was assessed by Agilent Bioanalyzer 2100 with conc. > 100 ng $μl^{-1}$, RNA integrity number > 7.0, OD260/280 > 1.8 and total RNA > 20 μg.

For the mRNA-Seq library, Poly(A) mRNA was isolated from total RNA using the NEBNext® Poly(A) mRNA Magnetic Isolation Module (NEB, E7490, San Diego, CA, USA), and the purified mRNA was used to construct the mRNA-Seq library following the

manufacturer's instructions for the NEBNext Ultra RNA Library Prep Kit (NEB, E7530, San Diego, CA, USA) and the NEBNext Multiplex Oligos (NEB, E7500, San Diego, CA, USA) from Illumina. The libraries were pooled and sequenced on a flow cell using an Illumina HiSeq™ 2500 sequencing platform.

For the sRNA-Seq library, 20 μg total RNA for each sample was resolved on 15% urea–polyacrylamide gel electrophoresis gel after denaturation, and gel slices corresponding to approximately 15–40-nt RNA fragments were separated. The RNA was precipitated by sodium acetate and ethanol, and used for sRNA library construction following instructions from the NEBNext Multiplex Small RNA Library Prep Set for Illumina® (NEB, E7300S, San Diego, CA, USA). The sRNA libraries were pooled and sequenced on an Illumina HiSeq 2500 platform at Beijing Biomarker Technology (Beijing, China) to produce 50-bp single-end reads. For library construction, 20 μg total RNAs was used to construct a degradome-Seq library. The library construction was performed based on a previously described method (German *et al.*, 2008).

mRNA-Seq data processing

FASTQC (http://www.bioinformatics.babraham.ac.uk/projects/fastqc/) was used for initial reads QC metrics (base quality distribution). NGS QC toolkits were used to trim adaptors and low-quality reads (Patel and Jain 2012). TE annotation was acquired from the Oryza Repeat Database (Ouyang and Buell, 2004). The clean reads were mapped to the rice reference genome (MSU_v7.0) using hisat2 V2.1.0 with default settings (Kim *et al.*, 2015). The bam files of uniquely mapped reads were used as inputs for the Stringtie (Pertea *et al.*, 2015), and transcripts per million reads values were calculated to measure the expression levels of genes. GO enrichment and binding factor enrichment analysis were carried out using the web-based Plant Regulomics (http://bioinfo.sibs.ac.cn/plant-regulomics; Ran *et al.*, 2020). The Venn diagrams and the heatmaps were shown using TBtools (Chen *et al.*, 2020).

sRNA-Seq data processing

After trimming adaptor sequences at the 5′- and 3′-ends of the sequenced reads, the trimmed reads aligned to cellular structural RNAs (e.g. rRNAs, snoRNAs, snRNAs) were removed using Bowtie v1.1.0 (Langmead *et al.*, 2009) with the parameters '-v 2 k1'. Clean reads of 18–30 nt were aligned to the rice genome using ShortStack v3.4 (Axtell, 2013) with parameters (--mismatches 0 --mmap u --bowtie_m 1000 --ranmax 50).

After removing sRNAs aligned to miRNAs, the remaining sRNA reads were then used to identify siRNA clusters. Only reads mapped to unique loci were counted for subsequent analyses. A siRNA cluster or locus was defined as a genomic region matched by at least three sRNA reads. If one cluster resided within 200 nt of another, they were merged and regarded as a single cluster. The expression levels of siRNA clusters were normalized to reads per million (RPM) that was calculated using the formula RPM = number of readcount/total mapped clean reads $\times 10^6$.

Phenotypic analysis and Fe content determination

Rice seedlings under Fe-sufficient or -deficient conditions were further supplied with 5-aza-2-deoxycytidine (+Aza) or without 5-aza-2-deoxycytidine (−Aza) by adding 20 μM 5-aza-2-deoxycytidine (if supplied) when the nutrient solution was renewed. After treatment, the roots were washed three times with 5 mM CaCl$_2$ solution and separated from the shoots with a razor (Sasaki *et al.*, 2014). Samples were dried at 70°C in an air-forced oven and

weighted. The dried samples were digested in 5 ml of 11 M HNO$_3$ for 5 h at 150°C. Fe concentration was then measured using an inductively coupled plasma-mass spectrometry (Agilent 7500ce, Palo Alto, CA, USA).

Bisulfite sequencing

To validate the effect of Fe-deficiency or Aza treatment on gene methylation level, three genes were randomly selected for bisulfate PCR assessment. DNA (1–500 ng) from each sample was treated with sodium bisulfate using EZ DNA Methylation-Gold kit (ZYMO Research, orange county, CA, USA) and amplified using specific primers designed by the web-based tool Methyl Primer Express v1.0 (http://www.urogene.org/cgi-bin/methprimer/methprimer.cgi). All primers used for bisulfite-reverse transcriptase-PCR (RT-PCR) are listed in Table S6. For each PCR reaction, 1 μl bisulfite-treated DNA was used in a 20-μl reaction. PCR products were purified using the Wizard SV Gel and PCR Clean-Up System Kit, and subcloned into the T-easy vector (Promega, Madison, WI, USA). The sequencing results were analyzed using software BiQ Analyzer (http://biq-analyzer.bioinf.mpi-inf.mpg.de/).

Real-time quantitative RT-PCR

A cDNA Synthesis Kit (TaKaRa, Dalian, China) was used to synthesize first-strand cDNA. Quantitative RT-PCR was performed using the SYBR Green Supermix system on a LightCycler 480 machine (Roche, Mannheim, Germany). Each sample was performed in three biological and three technical replications. The relative transcript levels were calculated using the $2^{-\Delta\Delta CT}$ method, and *OsActin* was used as the internal control to normalize the same samples. Primers are listed in Table S6.

Statistical analysis

In this study, statistical tests were used in a variety of comparisons as listed below.

(i) Differentially methylated cytosines (DMCs) were identified between Fe-sufficient and Fe-deficient samples by Benjamini–Hochberg FDR < 0.05 correction. DMRs were identified using Metilene (Jühling *et al.*, 2016) with minor modifications. A DMR was required to contain at least three DMCs with < 300 bp in distance between adjacent cytosine sites and coverage depth > 10 ×. In addition, CG DMRs, CHG DMRs and CHH DMR candidate regions with < 0.2, 0.1 and 0.1 differences between maximum and minimum methylation levels, respectively, were discarded. Finally, the regions with Fisher's exact test *P*-value < 0.05 and at least twofold change were determined as DMRs. Overlapping DMRs were concatenated.

i DEGs and TEs were determined using EdgeR (Robinson *et al.*, 2010) with a twofold change and a FDR < 0.05.
ii Differential expressed siRNA clusters were determined by DEseq2 (Love *et al.*, 2014) with a twofold change and a *P*-value < 0.05.
iii Methylation level and 24-nt siRNA abundance were calculated surrounding genes and TEs (in the 2-kb regions flanking to the expressed genes or TEs) based on sliding windows. The correlation of changes of DEGs with their nearby TEs (within 2 kb) and 24-nt siRNA clusters (within 2 kb) were determined with correlation coefficient (R^2), highly correlated was defined with *P* < 0.01.

AUTHOR CONTRIBUTIONS

SS and HS conceived and designed the research. JZ, SS and RG conducted the experiment. SS analyzed the data. SS, JW and HS wrote the manuscript. All authors read and approved the final manuscript.

CONFLICTS OF INTEREST

The authors declare that they have no competing interests.

DATA AVAILABILITY STATEMENT

The sequencing data generated in this study were deposited at the National Center for Biotechnology Information's Sequence Read Archive (SRA) under accession number PRJNA704534.

SUPPORTING INFORMATION

Additional Supporting Information may be found in the online version of this article.

Figure S1. Relative transcript abundance of *OsbHLH156*, *IRO2*, *NAAT1*, *NAS2* in shoots and roots of rice seedlings grown with 125 μM EDTA-Fe(II) (+Fe) or no Fe (−Fe) for 10 days. Data represent means ± standard deviation (SD), $n = 3$; *$P < 0.05$; **$P < 0.01$; ***$P < 0.001$; one-way analysis of variance (ANOVA) followed by Tukey test.

Figure S2. Relative transcript abundance of *HRZ1*, *NAAT1*, *NAS2* and *YSL15* in the rice roots. Data represent means ± SD, $n = 3$; *$P < 0.05$; **$P < 0.01$; ***$P < 0.001$; one-way analysis of variance (ANOVA) followed by Tukey test.

Table S1. MethylC sequencing information and mapping statistics

Table S2. The ratio of the number of reads of methylation sites supporting mCpG type detected

Table S3. Summary of Fe-deficiency-responsive DMRs in the rice roots and shoots

Table S4. Information of differentially methylated DEGs in the roots and shoots (supports Figure 4)

Table S5. Expression levels of genes relevant to DNA methylation in the rice roots and shoots under Fe/Pi-sufficient and -deficient conditions

Table S6. Primers used in this study

REFERENCES

Agius, F., Kapoor, A. & Zhu, J.-K. (2006) Role of the Arabidopsis DNA glycosylase/lyase ROS1 in active DNA demethylation. *Proceedings of the National Academy of Sciences of the United States of America*, **103**, 11796–11801.

Ahmad, F., Huang, X., Lan, H.X., Huma, T., Bao, Y.M., Huang, J. *et al.* (2014) Comprehensive gene expression analysis of the DNA (cytosine-5) methyltransferase family in rice (*Oryza sativa* L.). *Genetics and Molecular Research*, **13**, 5159–5172.

Axtell, M.J. (2013) ShortStack: comprehensive annotation and quantification of small RNA genes. *RNA*, **19**, 740–751.

Bartee, L., Malagnac, F. & Bender, J. (2001) Arabidopsis cmt3 chromomethylase mutations block non-CG methylation and silencing of an endogenous gene. *Genes and Development*, **15**, 1753–1758.

Bolger, A.M., Lohse, M. & Usadel, B. (2014) Trimmomatic: a flexible trimmer for Illumina sequence data. *Bioinformatics*, **30**, 2114–2120.

Bughio, N., Yamaguchi, H., Nishizawa, N.K., Nakanishi, H. & Mori, S. (2002) Cloning an iron-regulated metal transporter from rice. *Journal of Experimental Botany*, **53**, 1677–1682.

Chen, C., Chen, H., Zhang, Y., Thomas, H.R., Frank, M.H., He, Y. *et al.* (2020) TBtools: an integrative toolkit developed for interactive analyses of big biological data. *Molecular Plant*, **13**, 1194–1202.

Chen, X.C., Schonberger, B., Menz, J. & Ludewig, U. (2018) Plasticity of DNA methylation and gene expression under zinc deficiency in Arabidopsis roots. *Plant and Cell Physiology*, **59**, 1790–1802.

Chen, X. & Zhou, D.X. (2013) Rice epigenomics and epigenetics: challenges and opportunities. *Current Opinion in Plant Biology*, **16**, 164–169.

Cheng, L., Wang, F., Shou, H., Huang, F., Zheng, L., He, F. (2007) Mutation in nicotianamine aminotransferase stimulated the Fe(II) acquisition system and led to iron accumulation in rice. *Plant Physiology*, **145**, 1647–1657.

Chu, S., Zhang, X., Yu, K., Lv, L., Sun, C., Liu, X. *et al.* (2020) Genome-wide analysis reveals dynamic epigenomic differences in soybean response to low-phosphorus stress. *International Journal of Molecular Sciences*, **21**, 18.

Clark, M.A., Goheen, M.M. & Cerami, C. (2014) Influence of host iron status on *Plasmodium falciparum* infection. *Frontiers in Pharmacology*, **5**, 84.

Feng, S.J., Liu, X.S., Tao, H., Tan, S.K., Chu, S.S., Oono, Y. *et al.* (2016) Variation of DNA methylation patterns associated with gene expression in rice (*Oryza sativa*) exposed to cadmium. *Plant Cell and Environment*, **39**, 2629–2649.

German, M.A., Pillay, M., Jeong, D.H., Hetawal, A., Luo, S., Janardhanan, P. *et al.* (2008) Global identification of microRNA-target RNA pairs by parallel analysis of RNA ends. *Nature Biotechnology*, **26**, 941–946.

Guerinot, M.L. & Yi, Y. (1994) Iron: nutritious, noxious, and not readily available. *Plant Physiology*, **104**, 815–820.

Hansch, R. & Mendel, R.R. (2009) Physiological functions of mineral micronutrients (Cu, Zn, Mn, Fe, Ni, Mo, B, Cl). *Current Opinion in Plant Biology*, **12**, 259–266.

He, Y. & Ecker, J.R. (2015) Non-CG methylation in the human genome. *Annual Review of Genomics and Human Genetics*, **16**, 55–77.

Huff, J.T. & Zilberman, D. (2014) Dnmt1-independent CG methylation contributes to nucleosome positioning in diverse eukaryotes. *Cell*, **156**, 1286–1297.

Inoue, H., Higuchi, K., Takahashi, M., Nakanishi, H., Mori, S. & Nishizawa, N.K. (2003) Three rice nicotianamine synthase genes, OsNAS1, OsNAS2, and OsNAS3 are expressed in cells involved in long-distance transport of iron and differentially regulated by iron. *Plant Journal*, **36**, 366–381.

Inoue, H., Kobayashi, T., Nozoye, T., Takahashi, M., Kakei, Y., Suzuki, K. *et al.* (2009) Rice OsYSL15 is an iron-regulated iron(III)-deoxymugineic acid transporter expressed in the roots and is essential for iron uptake in early growth of the seedlings. *Journal of Biological Chemistry*, **284**, 3470–3479.

Ishimaru, Y., Suzuki, M., Tsukamoto, T., Suzuki, K., Nakazono, M., Kobayashi, T. *et al.* (2006) Rice plants take up iron as an Fe3+-phytosiderophore and as Fe2+. *Plant Journal*, **45**, 335–346.

Juhling, F., Kretzmer, H., Bernhart, S.H., Otto, C., Stadler, P.F. & Hoffmann, S. (2016) metilene: fast and sensitive calling of differentially methylated regions from bisulfite sequencing data. *Genome Research*, **26**, 256–262.

Kankel, M.W., Ramsey, D.E., Stokes, T.L., Flowers, S.K., Haag, J.R., Jeddeloh, J.A. *et al.* (2003) Arabidopsis MET1 cytosine methyltransferase mutants. *Genetics*, **163**, 1109–1122.

Kawashima, T. & Berger, F. (2014) Epigenetic reprogramming in plant sexual reproduction. *Nature Reviews in Genetics*, **15**, 613–624.

Kim, D., Landmead, B. & Salzberg, S.L. (2015) HISAT: a fast spliced aligner with low memory requirements. *Nature Medicine*, **12**, 357–360.

Kinoshita, T. & Seki, M. (2014) Epigenetic memory for stress response and adaptation in plants. *Plant Cell Physiology*, **55**, 1859–1863.

Kobayashi, T., Itai, R.N. & Nishizawa, N.K. (2014) Iron deficiency responses in rice roots. *Rice*, **7**, 11.

Kobayashi, T. & Nishizawa, N.K. (2012) Iron uptake, translocation, and regulation in higher plants. *Annual Review of Plant Biology*, **63**, 131–152.

Kobayashi, T., Nozoye, T. & Nishizawa, N.K. (2019) Iron transport and its regulation in plants. *Free Radical Biology and Medicine*, **133**, 11–20.

Kobayashi, T., Ogo, Y., Itai, R.N., Nakanishi, H., Takahashi, M., Mori, S. *et al.* (2007) The IDEF1 regulates the response to and tolerance of iron

deficiency in plants. *Proceedings of the National Academy of Sciences of the United States of America*, **104**, 19150–19155.

Krueger, F. & Andrews, S.R. (2011) Bismark: a flexible aligner and methylation caller for Bisulfite-Seq applications. *Bioinformatics*, **27**, 1571–1572.

Langmead, B., Trapnell, C., Pop, M. & Salzberg, S.L. (2009) Ultrafast and memory-efficient alignment of short DNA sequences to the human genome. *Genome Biology*, **10**, R25.

Law, J.A. & Jacobsen, S.E. (2010) Establishing, maintaining and modifying DNA methylation patterns in plants and animals. *Nature Reviews Genetics*, **11**, 204–220.

Li, X., Zhu, J.D., Hu, F.Y., Ge, S., Ye, M.Z., Xiang, H. *et al.* (2012) Single-base resolution maps of cultivated and wild rice methylomes and regulatory roles of DNA methylation in plant gene expression. *BMC Genomics*, **13**, 15.

Lindroth, A.M., Cao, X.F., Jackson, J.P., Zilberman, D., McCallum, C.M., Henikoff, S. *et al.* (2001) Requirement of CHROMOMETHYLASE3 for maintenance of CpXpG methylation. *Science*, **292**, 2077–2080.

Liu, J., Wu, X., Yao, X., Yu, R., Larkin, P.J. & Liu, C.M. (2018) Mutations in the DNA demethylase OsROS1 result in a thickened aleurone & improved nutritional value in rice grains. *Proceedings of the National Academy of Sciences of the United States of America*, **115**, 11327–11332.

Love, M.I., Huber, W. & Anders, S. (2014) Moderated estimation of fold change and dispersion for RNA-seq data with DESeq2. *Genome Biology*, **15**, 550.

Martinez, G., Panda, K., Kohler, C. & Slotkin, R.K. (2016) Silencing in sperm cells is directed by RNA movement from the surrounding nurse cell. *Nature Plants*, **2**, 16030.

Matzke, M.A., Kanno, T. & Matzke, A.J.M. (2015) RNA-directed DNA methylation: the evolution of a complex epigenetic pathway in flowering plants. *Annual Review of Plant Biology*, **66**, 243–267.

Matzke, M.A. & Mosher, R.A. (2014) RNA-directed DNA methylation: an epigenetic pathway of increasing complexity. *Nature Reviews Genetics*, **15**, 394–408.

Mirouze, M. & Paszkowski, J. (2011) Epigenetic contribution to stress adaptation in plants. *Current Opinion in Plant Biology*, **14**, 267–274.

Molnar, A., Melnyk, C.W., Bassett, A., Hardcastle, T.J., Dunn, R. & Baulcombe, D.C. (2010) Small silencing RNAs in plants are mobile and direct epigenetic modification in recipient cells. *Science*, **328**, 872–875.

Mosher, R.A. & Melnyk, C.W. (2010) siRNAs and DNA methylation: seedy epigenetics. *Trends in Plant Science*, **15**, 204–210.

Nuthikattu, S., McCue, A.D., Panda, K., Fultz, D., DeFraia, C., Thomas, E.N. *et al.* (2013) The initiation of epigenetic silencing of active transposable elements is triggered by RDR6 and 21–22 nucleotide small interfering RNAs. *Plant Physiology*, **162**, 116–131.

Ogo, Y., Itai, R.N., Nakanishi, H., Inoue, H., Kobayashi, T., Suzuki, M. *et al.* (2006) Isolation and characterization of IRO2, a novel iron-regulated bHLH transcription factor in graminaceous plants. *Journal of Experimental Botany*, **57**, 2867–2878.

Ogo, Y., Kobayashi, T., Itai, R.N., Nakanishi, H., Kakei, Y., Takahashi, M. *et al.* (2008) A novel NAC transcription factor, IDEF2, that recognizes the iron deficiency-responsive element 2 regulates the genes involved in iron homeostasis in plants. *Journal of Biological Chemistry*, **283**, 13407–13417.

Ortega-Galisteo, A.P., Morales-Ruiz, T., Ariza, R.R. & Roldan-Arjona, T. (2008) Arabidopsis DEMETER-LIKE proteins DML2 and DML3 are required for appropriate distribution of DNA methylation marks. *Plant Molecular Biology*, **67**, 671–681.

Ouyang, S. & Buell, C.R. (2004) The TIGR plant repeat databases: a collective resource for the identification of repetitive sequences in plants. *Nucleic Acids Research*, **32**, D360–D363.

Pagliarani, C. & Gambino, G. (2019) Small RNA mobility: spread of RNA silencing effectors and its effect on developmental processes and stress adaptation in plants. *International Journal of Molecular Science*, **20**, 19.

Parent, J.S., Bouteiller, N., Elmayan, T. & Vaucheret, H. (2015) Respective contributions of Arabidopsis DCL2 and DCL4 to RNA silencing. *Plant Journal*, **81**, 223–232.

Park, E.Y., Tsuyuki, K.M., Hu, F., Lee, J. & Jeong, J. (2019) PRC2-mediated H3K27me3 contributes to transcriptional regulation of FIT-dependent iron deficiency response. *Frontiers in Plant Science*, **10**, 627.

Patel, R.K. & Jain, M. (2012) NGS QC toolkit: A toolkit for quality control of next generation sequencing data. *PLoS One*, **7**, 7.

Penterman, J., Zilberman, D., Huh, J.H., Ballinger, T., Henikoff, S. & Fischer, R.L. (2007) DNA demethylation in the Arabidopsis genome. *Proceedings of the National Academy of Sciences of the United States of America*, **104**, 6752–6757.

Pertea, M., Pertea, G.M., Antonescu, C.M., Chang, T.C., Mendell, J.T. & Salzberg, S.L. (2015) StringTie enables improved reconstruction of a transcriptome from RNA-seq reads. *Nature Biotechnology*, **33**, 290–295.

Qian, Y., Xi, Y., Cheng, B. & Zhu, S. (2014) Genome-wide identification and expression profiling of DNA methyltransferase gene family in maize. *Plant Cell Report*, **33**, 1661–1672.

Ran, X., Zhao, F., Wang, Y., Liu, J., Zhuang, Y., Ye, L. *et al.* (2020) Plant regulomics: a data-driven interface for retrieving upstream regulators from plant multi-omics data. *Plant Journal*, **101**, 237–248.

Robinson, M.D., McCarthy, D.J. & Smyth, G.K. (2010) edgeR: a bioconductor package for differential expression analysis of digital gene expression data. *Bioinformatics*, **26**, 139–140.

Rodrigues, J.A. & Zilberman, D. (2015) Evolution and function of genomic imprinting in plants. *Genes and Development*, **29**, 2517–2531.

Sankaran, V.G. & Weiss, M.J. (2015) Anemia: progress in molecular mechanisms and therapies. *Nature Medicine*, **21**, 221–230.

Sasaki, A., Yamaji, N. & Ma, J.F. (2014) Overexpression of OsHMA3 enhances Cd tolerance and expression of Zn transporter genes in rice. *Journal of Experimental Botany*, **65**, 6013–6021.

Schmitz, R.J., Lewis, Z.A. & Goll, M.G. (2019) DNA methylation: shared and divergent features across eukaryotes. *Trends in Genetics*, **35**, 818–827.

Secco, D., Wang, C., Shou, H.X., Schultz, M.D., Chiarenza, S., Nussaume, L. *et al.* (2015) Stress induced gene expression drives transient DNA methylation changes at adjacent repetitive elements. *Elife*, **4**, 26.

Tamiru, M., Hardcastle, T.J. & Lewsey, M.G. (2018) Regulation of genome-wide DNA methylation by mobile small RNAs. *New Phytologist*, **217**, 540–546.

Tan, F., Zhou, C., Zhou, Q., Zhou, S., Yang, W., Zhao, Y. *et al.* (2016) Analysis of chromatin regulators reveals specific features of rice DNA methylation pathways. *Plant Physiology*, **171**, 2041–2054.

Teerawanichpan, P., Chandrasekharan, M.B., Jiang, Y., Narangajavana, J. & Hall, T.C. (2004) Characterization of two rice DNA methyltransferase genes and RNAi-mediated reactivation of a silenced transgene in rice callus. *Planta*, **218**, 337–349.

Wambui Mbichi, R., Wang, Q.F. & Wan, T. (2020) RNA directed DNA methylation and seed plant genome evolution. *Plant Cell Report*, **39**, 983–996.

Wang, L., Ying, Y., Narsai, R., Ye, L., Zheng, L., Tian, J. *et al.* (2013) Identification of OsbHLH133 as a regulator of iron distribution between roots and shoots in *Oryza sativa*. *Plant Cell and Environment*, **36**, 224–236.

Wang, N.N., Zhang, D., Wang, Z.H., Xun, H.W., Ma, J., Wang, H. *et al.* (2014) Mutation of the RDR1 gene caused genome-wide changes in gene expression, regional variation in small RNA clusters and localized alteration in DNA methylation in rice. *BMC Plant Biology*, **14**, 12.

Wang, S.D., Li, L., Ying, Y.H., Wang, J., Shao, J.F., Yamaji, N. *et al.* (2020) A transcription factor OsbHLH156 regulates Strategy II iron acquisition through localising IRO2 to the nucleus in rice. *New Phytologist*, **225**, 1247–1260.

Yamauchi, T., Johzuka-Hisatomi, Y., Fukada-Tanaka, S., Terada, R., Nakamura, I. & Iida, S. (2009) Homologous recombination-mediated knock-in targeting of the MET1a gene for a maintenance DNA methyltransferase reproducibly reveals dosage-dependent spatiotemporal gene expression in rice. *Plant Journal*, **60**, 386–396.

Yamauchi, T., Moritoh, S., Johzuka-Hisatomi, Y., Ono, A., Terada, R., Nakamura, I. *et al.* (2008) Alternative splicing of the rice OsMET1 genes encoding maintenance DNA methyltransferase. *J Plant Physiology*, **165**, 1774–1782.

Zhang, H., Lang, Z. & Zhu, J.K. (2018) Dynamics and function of DNA methylation in plants. *Nature Reviews Molecular Cell Biology*, **19**, 489–506.

Zhang, H. & Zhu, J.K. (2011) RNA-directed DNA methylation. *Current Opinion in Plant Biology*, **14**, 142–147.

Zheng, L.Q., Ying, Y.H., Wang, L., Wang, F., Whelan, J. & Shou, H.X. (2010) Identification of a novel iron regulated basic helix-loop-helix protein involved in Fe homeostasis in *Oryza sativa*. *BMC Plant Biology*, **10**, 9.